ISSN: 0067-2904

Study of Adsorption and Release Kinetics of Ciprofloxacin Drug on Prepared γ-Mesoporous Alumina

Hayder J. Mohammed [1 *] , Sameer H. Kareem[2]
[1] *Scientific Research Commission, Baghdad, Iraq*
[2]*Department of Chemistry - College of Science for women , University of Baghdad , Iraq*

Received: 25/1/2025 Accepted: 11/8/2025 Published: 30/ 7/2026

Abstract

This study focuses on the adsorption and release kinetics of the antibiotic ciprofloxacin (CIP) using previously synthesized γ- Mesoporous Alumina (γ-MA). The experiments of the adsorption kinetic study were carried out by batch method for 240 min, while release kinetics study were carried out via a dialysis bag method maintained at 37 °C with continuous magnetic stirring. The adsorption kinetics analysis was performed using three kinetics models: pseudo 1st order, pseudo 2nd order and intraparticle diffusion. Results indicating that the CIP adsorption is pseudo-2nd order reaction according to the values of correlation coefficient (R^2) for the linear graphs. The intraparticle diffusion model revealed a two-step adsorption mechanism: the first linear section is responsible to the CIP molecules' diffusion between particles and the second linear section is the diffusion that occurs within tiny pores. Also, the release kinetics analysis performed using three kinetics models the Korsmeyer – Peppas, 1st order, and Kopcha, and the findings indicate that the Korsmeyer-Peppas model provided the most accurate fit to the data on releasing kinetics, and values of n suggest that non-Fickian and Fickian diffusion governs the kinetics of CIP release from γ-MA in pH 7 and pH 5 media respectively. Drug loading investigation showed CIP loaded of 2.82 mg per gram of γ-MA. The release profile for CIP loaded on γ-MA (CIP/γ-MA) system shows that the drug release percentage after 1560 min (26 hours) was about 51.47 % in pH 7 media, and about 35.29 % in pH 5 media.

Keywords: Mesoporous Alumina; Ciprofloxacin; Adsorption; Loading; Drug release.

دراسة حركية الامتزاز والاطلاق لدواء سيبروفلوكساسين على الالومينا متوسطة المسام المحضرة

حيدر جاسم محمد[1] , سمير حكيم كريم[2]
[1] هيئة البحث العلمي , بغداد, العراق
[2] قسم الكيمياء,كلية العلوم للبنات, جامعة بغداد, بغداد, العراق

*Email: Haidar.Jassem2305@sc.uobaghdad.edu.iq

الخلاصة

تُركز هذه الدراسة على حركية الامتزاز والانطلاق للمضاد الحيوي سيبروفلوكساسين (CIP) باستخدام الالومينا متوسطة المسام (γ–MA) المُصنّعة مسبقًا. أُجريت تجارب دراسة حركية الامتزاز بطريقة الدفعات لمدة 240 دقيقة، بينما أُجريت دراسة حركية الانطلاق بطريقة كيس الديلزة المُحافظ عليه عند درجة حرارة 37 درجة مئوية مع التحريك المغناطيسي المستمر. أُجري تحليل حركية الامتزاز باستخدام ثلاثة نماذج حركية: المرتبة الاولى الكاذبة والمرتبة الثانية الكاذبة والانتشار داخل الجسيمات. تُشير النتائج إلى أن امتزاز CIP هو تفاعل المرتبة الثانية الكاذبة وفقًا لقيم معامل الارتباط (R2) للرسوم البيانية الخطية. كشف نموذج الانتشار داخل الجسيمات عن آلية امتزاز من خطوتين: القسم الخطي الأول مسؤول عن انتشار جزيئات CIP بين الجسيمات، والقسم الخطي الثاني هو الانتشار الذي يحدث داخل المسام الدقيقة. كما أُجري تحليل حركية الإطلاق باستخدام ثلاثة نماذج حركية: نموذج Korsmeyer–Peppas والمرتبة الاولى وKopcha. وتشير النتائج إلى أن نموذج Korsmeyer–Peppas وفّر أدقّ توافق مع بيانات حركية الإطلاق، وتشير قيم n إلى أن الانتشار non–Fickian و Fickian يتحكمان في حركية إطلاق CIP من γ–MA في أوساط ذات الرقم الهيدروجيني 7 و5 على التوالي. أظهر فحص تحميل الدواء أن CIP محمل بـ 2.82 ملغ لكل غرام من. γ– MA يُظهر ملف تعريف الإطلاق لـ CIP المحمل على نظام (CIP/γ–MA) γ–MA أن نسبة إطلاق الدواء بعد 1560 دقيقة (26 ساعة) كانت حوالي 51.47% في الوسائط ذات الرقم الهيدروجيني 7، وحوالي 35.29% في الوسائط ذات الرقم الهيدروجيني 5.

1. Introduction

Mesoporous materials are a significant focus of research in the modern scientific community. Their large surface area and adjustable pore architecture render those distinctive in ushering a new epoch in contemporary nanotechnology [1]. These materials have diverse applications across various sectors, including catalysis, gas detection, electronics industry, etc. [2]. The medicinal purposes of these substances are essential for developing nanomedicine and disparity agents for magnetic resonance imaging procedures. A primary priority in contemporary research is the synthesis of mesoporous material-based drug delivery systems to mitigate the adverse side effects of pharmaceuticals [3]. The successfully prepared γ-MA showed unique properties such as controlled porosity, high thermal and mechanical stability, chemical inertness, and tunable surface chemistry, which has made γ-MA an excellent host for extensive drug loading and controlled release (drug delivery) in an area of biomedicine [4-6]. CIP is a prominent fluoroquinolone and the most extensively utilized chemotherapeutic antibiotic globally. [7, 8]. CIP is primarily utilized in human medication, particularly for the treatment of urinary tract infections in males [9, 10]. Figure 1 illustrates the chemical structure of this drug.

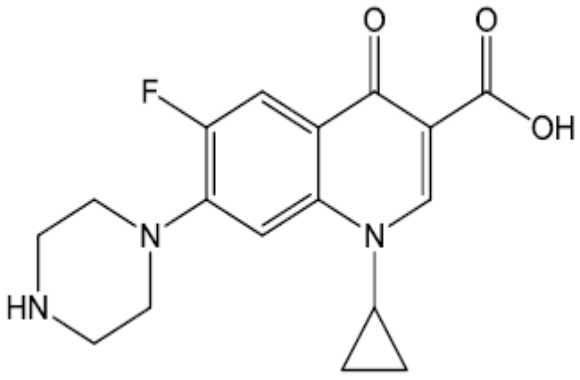

Figure 1 : Chemical structure of CIP drug.

Ewelina Weidner et al [11], prepared Al_2O_3/La_2O_3, and examined its structural properties as well as its and application as a diclofenac delivery system were investigated. At pH 7.2 and 1.2, the release was 50% and 80% of diclofenac respectively, this indicates the potential use of the engineered material as a novel carrier for the prolonged release of several active medicinal components. Maria Porta-i-Batalla et al [12], fabricated nanoporous anodic Alumina (NAA) and the drug delivery rates were analyzed utilizing doxorubicin as a model medicine. The findings indicate effective modelling of all 3D pore structures, distinguishing between two stages of drug release. So, the Higuchi and Korsmeyer-Peppas equations effectively modelled both for short and long release time. B. Shree Haripriya et al [13], Fabricated silver nanoparticles, immobilized on mesoporous Santa Barbara Amorphous-15 (SBA-15), functionalized with 3-glycidoxypropyl trimethoxy silane, and then treated with tris(2-aminoethyl)amine (SBA-15/GPTMS-TAEA-Ag). The prepared SBA-15/GPTMS-TAEA-Ag served as a delivery system for CIP. In vitro investigation revealed that the loading and release of CIP were 19.8% and 98.14% of the initially loaded CIP, respectively.
In earlier studies, magnetic iron oxide mesoporous silica material (Fe_3O_4@$mSiO_2$) [14] and mesoporous silica nanoparticles [15] have been utilized as a carrier for CIP delivery. Therefore, the current research focuses on evaluating the loading capacity and release profile of CIP using laboratory-prepared γ-MA. Loading was performed using the adsorption method while releasing it using a dialysis bag with a pH 7.4 and 5.4 buffer solution. The study also includes the kinetics investigation of adsorption and release.

2. Materials and methods

2.1. The carriers:

The procedure used for γ-MA preparation is a modified procedure reported in reference [16], and as follows: 2.3 g sodium dodecyl sulfate (SDS) (CH_3 $(CH_2)_{11}OSO_3Na$ (obtained from the state company of vegetable oils – Iraq, purity >98%) was dissolved in 100 mL of deionized water (solution A), and 17.12 g $Al_2(SO_4)_3$ (obtained from Panreac Química, purity=99%) solve in 100 milliliters of distilled water (solution B). Subsequently, solution B was added to solution A drop by drop while stirring to 30 min. at 70 °C. Solution pH was then adjusted to 9 by adding ammonia solution (25%) from ACI Labscan incrementally and agitated to create white suspensions for about 120 minutes at 70 °C. The formed solution was placed into a water bath at 70 °C and for 20 hr until converted into a gel. This product was filtered, rinsed repeatedly by distilled water, dried in an oven set at 80 °C for eight hours, and calcined at 550 °C for 4h.

The synthesized γ-MA exhibits a crystalline structure with cubic symmetry; the particle size distribution was in the range (10-55 nm), surface area 400.8 m^2g^{-1}, pore volume 0.8971 cm^3g^{-1} and average pore diameter 8.95 nm. Further details regarding its characterization will be available in reference [17].

2.2. Batch method for adsorption kinetic

The experiments of kinetic study were carried out in a 250 mL conical flask that included 0.3 g of γ-MA and 100 mL of 6 $mg.L^{-1}$ CIP drug. A water bath shaker operating at 200 rpm was used to agitate the solutions during the experiments for 240 min, which were conducted at 25 °C. After interval time, the drug concentration is ascertainable with a UV-vis spectrophotometer by Evaluation the absorbance at λ_{max} 276 nm.
The amount adsorbed q_e ($mg.g^{-1}$) was estimated utilizing the subsequent equation:

$$qe = \frac{(Co - Ce)\,V}{m} \quad (1)$$

Where C_o ($mg.L^{-1}$) is starting concentration of drug, C_e ($mg.L^{-1}$) is the equilibrium concentration of the drug, m is the γ-MA weight, and V is the adsorbate solution's volume in L [14].

2.3. Loading

The medicinal product was loaded onto the carriers via impregnation method: 15 mL of 30 $mg.L^{-1}$ solutions of the drug was added to the 0.3 g γ-MA carrier, and the mixture was then stirred magnetically for 24 hours to achieve equilibrium. The resulting solution was filtrated, and the resulting liquid phase was removed into a quartz cell to determine the amount of CIP using the UV-vis spectrophotometer. After that, the drug-loaded mesoporous composite was oven-dried for 12 hours at 50°C [15, 18].

2.4. In vitro release experiment

It was carried out according to the following; a dialysis bag containing of drug-loaded γ-MA with 2mL of buffer saline solution, pH 7.4 or 5.4, was soaked in the 18 mL of the saline solution and maintained at 37 °C under constant magnetic stirring (150 rpm). One milliliter samples were withdrawn at prearranged intervals (30,60,120,180,240,300,360,420,480,1080,1320,1560 minutes) and replaced with fresh phosphate buffer saline (PBS), and the drug concentration in the liquid phase was evaluated using a UV-vis spectrophotometer [15, 18].

3. Results and discussion

3.1. Adsorption Kinetics of CIP Hydrochloride

The kinetics of CIP adsorption was investigated by three models: pseudo first order, pseudo-second order, and intraparticle diffusion models. The difference between time-dependent intake (q_t) and equilibrium intake (q_e) in the pseudo-first-order equation is represented as a linear function of adsorption time spent (t), which is provided by equation 2 [19]:

$$ln(q_e - q_t) = ln\, q_e - k_1 t \quad (2)$$

The rate of adsorption is calculated using the following pseudo 2nd order reported in equation 3 [19]:

$$t \,/\, q_t = 1 \,/\, k_2 q_e^2 + t \,/\, q_e \quad (3)$$

Weber–Morris model was applied to specify the diffusion's mechanism and the slowest step [20-22]. It is illustrated in the equation 4:

$$q_t = k_D t^{1/2} + C \quad (4)$$

where k_1 is the rate constant of 1st order, k_2 is the rate constant of 2nd order, k_D is the diffusion's rate constant, and C is plot's intercept.

The experimental kinetic data obtained for the adsorption of CIP on γ-MA were fitted with the three models depicted in Figure 2. A comparison between the three models were applied. Table 1 displays all of the parameters and regression coefficients for the kinetic models mentioned above.

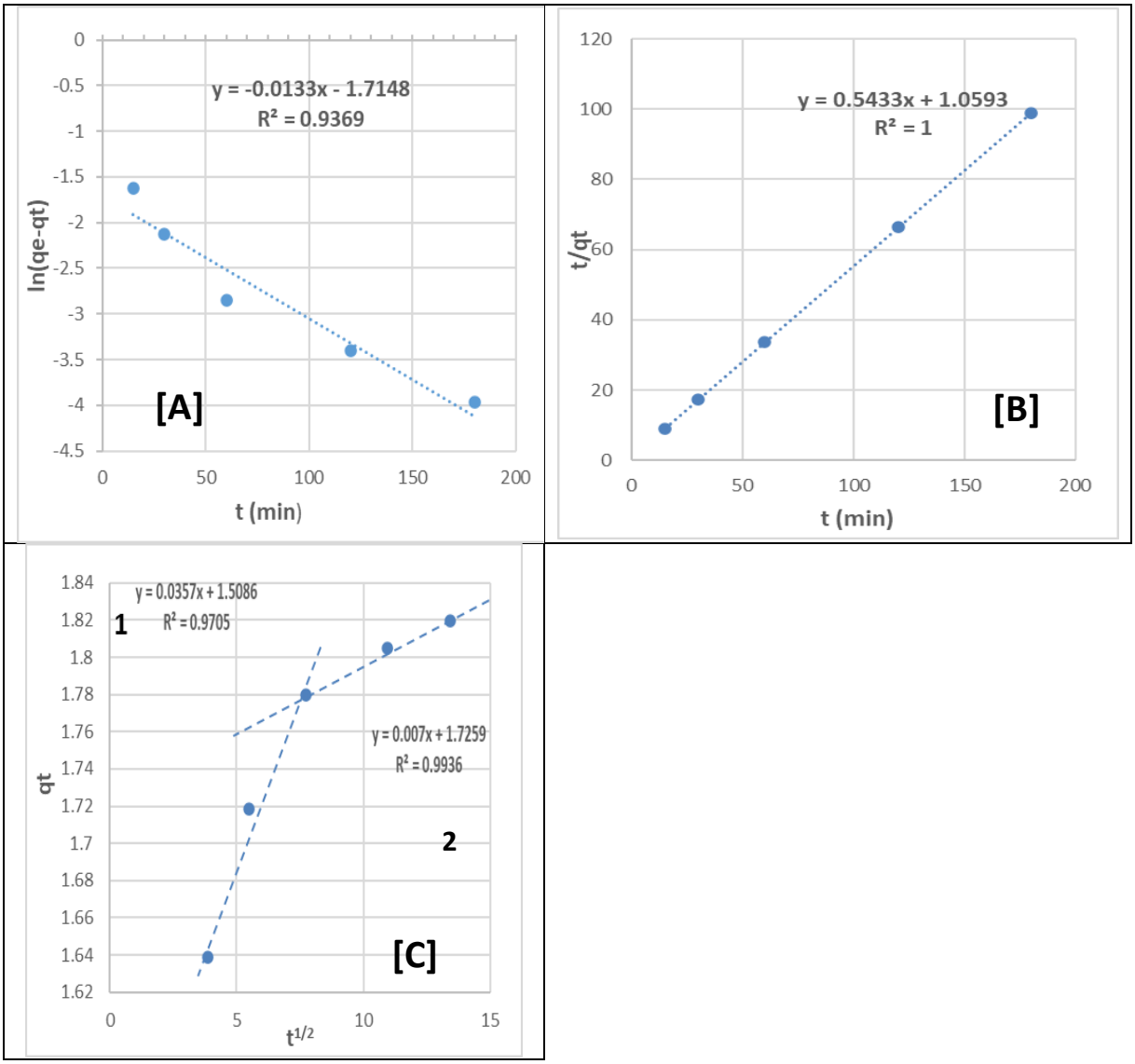

Figure 2 : Linear plots of the A) Pseudo first order, B) Pseudo second C) Intra-particles diffusion kinetics models for CIP adsorption on γ-MA

Table 1 : Kinetics functions of CIP medicine adsorption onto γ-MA

Model	Parameters	Value
pseudo-1st order	q_e (exp)	1.8581
	q_e (cal) (mg.g^{-1})	0.1799
	k_1(min)$^{-1}$	0.0133
	R^2	0.9369
pseudo-2nd order	q_e (cal) (mg.g^{-1})	1.841
	k_2 (g/mg/min)	0.2787
	R^2	1
Intraparticle diffusion	K_{D1} (mg/g·min$^{1/2}$)	0.0357
	$R^2$1	0.9705
	K_{D2}(mg/g·min$^{1/2}$)	0.007
	$R^2$2	0.9936

Based on the results presented in Table 1, the pseudo-second-order model demonstrated an excellent fit for the adsorption of CIP on the γ-MA with correlation coefficients equal 1, which proved the experimental data matches up by pseudo 2nd order kinetic approach. This

confirms that the experimental data align perfectly with the pseudo-second-order kinetic model.

The intra-particle equation can be used to identify the rate-determining step in diffusion. This model reflects that pore diffusion occurs due to the porous nature of adsorbent. If the regression of q_t versus $t^{1/2}$ passes through the origin, then intra-particle diffusion can be identified as a rate-controlling step [23, 24]. It can be showed from the plot of intra-particle diffusion equation; the adsorption process was governed by two steps. The first linear step is due to the diffusion of CIP molecules between particles (intra-particle diffusion). The second linear step is the diffusion inside small pores and then the equilibrium is established. If the data show multiple linear segments in the plots that do not intersect the origin, the rate-controlling step involves not just intra-particle diffusion but also more additional stages [25, 15].

3.2. Release Kinetics of CIP.

To obtain the release profiles of pharmaceuticals, a small amount of drug-loaded carriers can be placed in a large volume of release medium using a dialysis bag. CIP was incorporated into carriers for the in vitro examination of drugs release, and the subsequent expression was used to determine the quantity of drug-loaded by using equation 5. [26, 15]:

$$Loading\left(\frac{mg\ drug}{g\ sample}\right) = \frac{m\ orig - m\ solu}{m\ MPS} \quad (5)$$

Where m_{orig} is milligrams of CIP in the solution before impregnation and m_{solu} is milligrams of CIP in the solution after impregnation and m_{MPS} is the grams of the pure carrier. The determinate quantity of CIP medicine loaded in the carrier were 2.82 milligrams of the drug in a gram of carrier. These loading values are consistent with the capacity of other adsorbents-drugs defined by previous studies [26, 15].

In this study, drug release behavior was investigated at 37 °C, and pH= 7.4 and 5.4 (physiological condition), and the cumulative CIP release were shown in Figure 3.

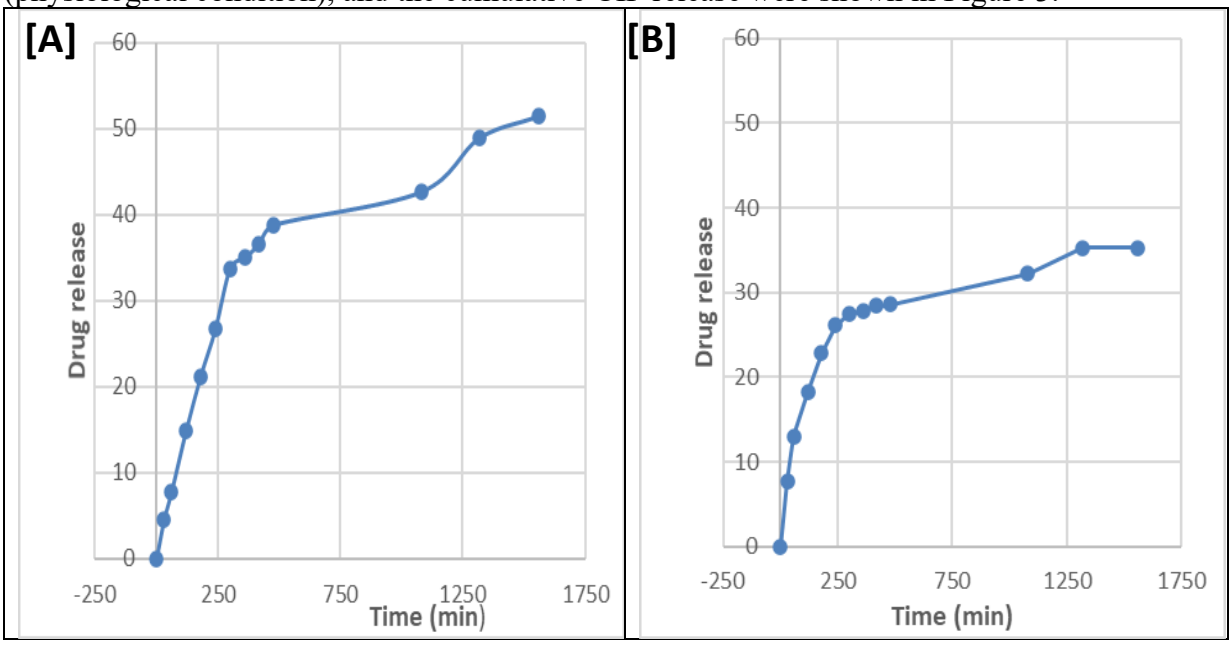

Figure 3 : The releasing profile of CIP drug loaded γ-MA at A) pH 7.4 and B) 5.4 For the CIP/γ-MA system, at pH 7.4, 51.47 % of loaded CIP released at condition decreased to 35.29 % at pH 5.4 after 1560 min. The lower amount of CIP released at lower pH values had been assign to low solubility of the medicine in this condition [27].

The data on drug release was entered into three kinetic models: Korsmeyer – Peppas (equation 6), pseudo-first-order (equation 7) and Kopcha Kinetics (equation 8) of CIP release from the carriers and the linear plots were illustrated in 4 and the results listed in table 3.

$$M_t / M_\infty = K_{k-p} t^n \quad (6)$$

$$M_t / M_\infty = 1 - e^{-kt} \quad (7)$$

$$M_t = At^{1/2} + Bt \quad (8)$$

In this case, M_t is the quantity of CIP released in minutes at time t, M∞ is the drug loaded in γ-MA particulates, $K_{K\text{-}P}$ is a kinetic constant associated with the host-guest couple, n is associated with the host's form and mechanism of drug release, and k is first order rate constant. A is the contribution of diffusion, and B is the contribution of erosion.

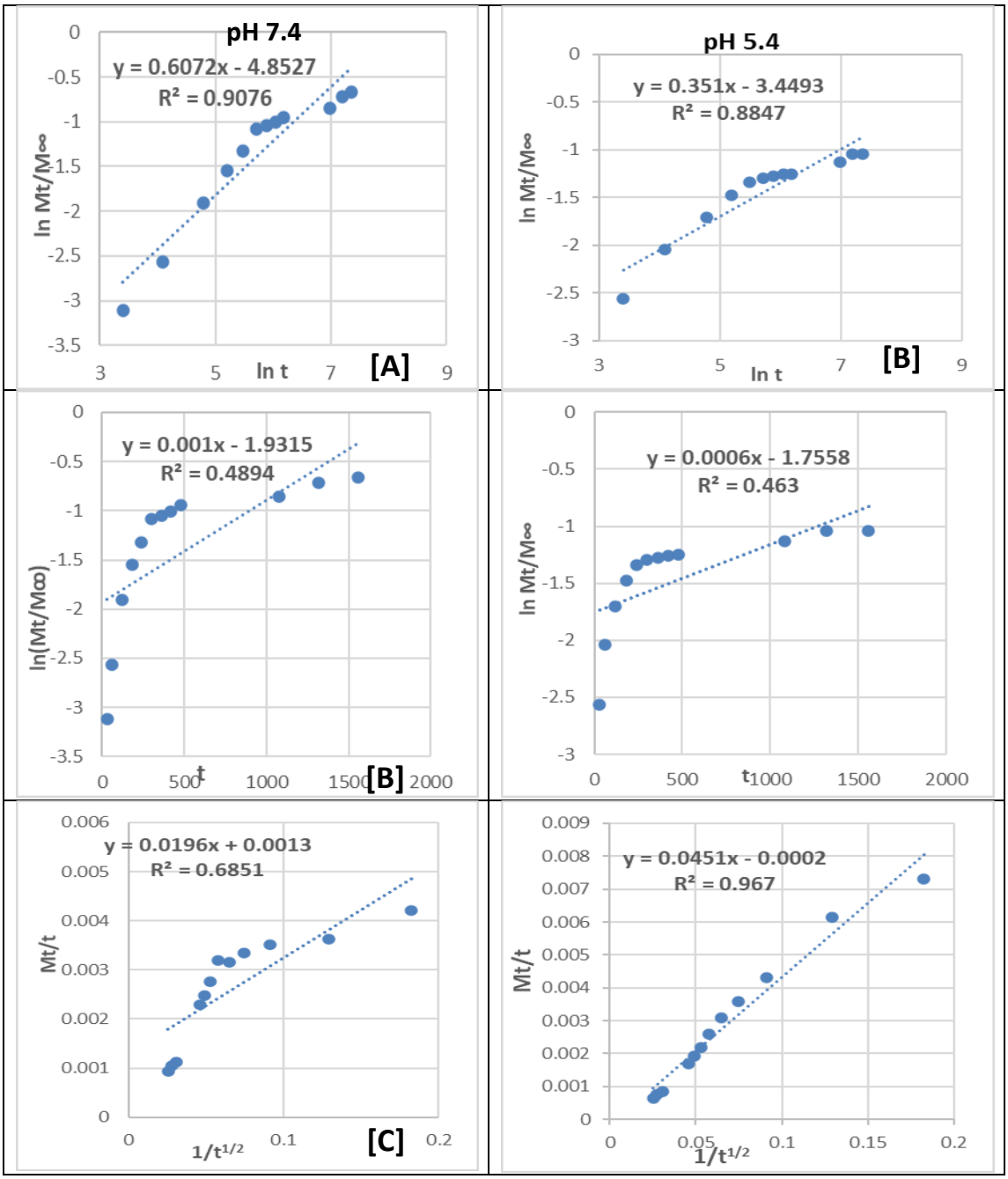

Figure 4 : The linear plots of; A) Korsmeyer- Peppas, B) pseudo First-order, and C) Kopcha models of kinetic release from γ-MA at pH 7.4 and 5.4 respectively.

Table 2 : The kinetics parameters of the release of CIP drug

model	Korsmeyer-peppas model			Pseudo-first -order		Kopcha model		
parameters	n	k_{K-P}	R^2	k	R^2	A	B	R^2
pH 7.4	0.607	0.0078	0.9076	0.001	0.4894	0.0196	0.0013	0.6851
pH 5.4	0.351	0.0318	0.8847	0.0006	0.463	0.0451	0.0002	0.967

The R^2 values for the release data at pH 5.4 indicated that the Peppas and Kopcha models provided the best fit for all systems. However, at 7.4, the results did not adequately fit the data, and the first kinetic model did not match the experimental data. The Peppas model displayed a value of n of 0.607 and 0.351 for pH 7.4 and 5.4 respectively, indicating that drug release at pH 7.4 was non-Fickian diffusion, whereas at pH 5.4, the release was Fickian diffusion. The Fickian diffusion mechanism controls the release when $n \leq 0.5$; While unusual diffusion (non-Fickian) mechanism governs the release when n ranges from 0.5 to 1; and the complex mechanism of transport governs the release when $n > 1$. This result is confined to other works. In the Kopcha approach, erosion is dominant when A/B less than one, whereas diffusion dominates when A/B equal or more than one 1. The results show that all the values of the two systems at the two pH 5.4 and 7.4 are more significant than 1, which shows diffusion as the dominant mechanism [28-31].

Conclusion

The key conclusions drawn from the study of adsorption and release kinetics of CIP on γ-MA are summarized as follows:

1. The results of adsorption kinetics examination show the adsorption of CIP medicine on γ-MA completely obeys by pseudo- 2nd order equation.
2. CIP drug-loaded γ-MA has a capacity of 2.40 mg drug/g carrier and the percent of CIP releasing after 1560 min in pH 7 and in pH 5 media for CIP/γ-MA system are 51.47 % and 35.29% respectively .
3. The release kinetics indicate that the Korsmeyer - Peppas model conforms more closely to the release data for CIP drug at CIP/γ-MA system.

Conflict of Interest

Conflicts of interest are not present, according to the authors.

Acknowledgment

The authors would like to thanks the college of science, University of Baghdad for presenting this work.

References

[1] M. Alem, A. Tarlani, and H. R. Aghabozorg, "Synthesis of nanostructured alumina with ultrahigh pore volume for pH-dependent release of curcumin," *RSC Advances*, vol. 7, no. 62, pp. 38935–38944, 2017.

[2] P. Singh and K. Sen, "Contemporary mesoporous materials for drug delivery applications: a review," *Journal of Porous Materials*, vol. 25, no. 4, pp. 965–987, 2018.

[3] S. Sim and N. K. Wong, "Nanotechnology and its use in imaging and drug delivery (Review)," *Biomedical reports*, vol. 14, no. 5, p. 42, 2021.

[4] P. F. Fulvio, R. I. Brosey, and M. Jaroniec, "Synthesis of mesoporous alumina from boehmite in the presence of triblock copolymer," *ACS applied materials & interfaces*, vol. 2, no. 2, pp. 588–593, 2010.

[5] M. Pourmadadi *et al.*, "Porous alumina as potential nanostructures for drug delivery applications, synthesis and characteristics," *Journal of Drug Delivery Science and Technology*,

vol. 77, no. 103877, p. 103877, 2022.

[6] S. H. Lakade, M. T. Harde, and P. K. Deshmukh, "Synthesis of mesoporous alumina: an impact of surface chemistry on release behavior," *Particulate Science and Technology*, pp. 1–7, 2019.

[7] L. J. M. Githinji, M. K. Musey, and R. O. Ankumah, "Evaluation of the fate of ciprofloxacin and amoxicillin in domestic wastewater," *Water, Air, & Soil Pollution*, vol. 219, no. 1–4, pp. 191–201, 2011.

[8] C. A. Aggelopoulos, M. Hatzisymeon, D. Tataraki, and G. Rassias, "Remediation of ciprofloxacin-contaminated soil by nanosecond pulsed dielectric barrier discharge plasma: Influencing factors and degradation mechanisms," *Chemical Engineering Journal*, vol. 393, no. 124768, p. 124768, 2020.

[9] A. Smart *et al.*, "Sniffing out resistance - Rapid identification of urinary tract infection-causing bacteria and their antibiotic susceptibility using volatile metabolite profiles," *Journal of pharmaceutical and biomedical analysis*, vol. 167, pp. 59–65, 2019.

[10] F. Wagenlehner *et al.*, "Explorative randomized phase II clinical study of the efficacy and safety of finafloxacin versus ciprofloxacin for treatment of complicated urinary tract infections," *Antimicrobial agents and chemotherapy*, vol. 62, no. 4, 2018.

[11] E. Weidner, P. Bartczak, J. Goscianska, T. Jesionowski, M. Jaroniec, and F. Ciesielczyk, "Soft-templating synthesis of mesoporous alumina enriched with lanthana and its potential as diclofenac delivery system," *Microporous and Mesoporous Materials*, vol. 351, no. 112487, p. 112487, 2023.

[12] M. Porta-i-Batalla, E. Xifré-Pérez, C. Eckstein, J. Ferré-Borrull, and L. Marsal, "3D nanoporous anodic alumina structures for sustained drug release," *Nanomaterials (Basel)*, vol. 7, no. 8, p. 227, 2017.

[13] B. Shree Haripriya, D. R. Anakha, R. Yamuna, M. Vinoba, and M. Bhagiyalakshmi, "Green synthesized AgNPs using Clitoria ternatea extract and its confinement on SBA-15/GPTMS-TAEA for controlled drug release of ciprofloxacin," *Journal of Porous Materials*, vol. 31, no. 1, pp. 351–363, 2024.

[14] S. H. Kareem, "Magnetic mesoporous silica material (Fe_3O_4@$mSiO_2$) as adsorbent and delivery system for ciprofloxacin drug," in *IOP Conference Series: Materials Science and Engineering*, vol. 871, IOP Publishing, 2020.

[15] M. A. Sachit and S. H. Kareem, "Isotherms and thermodynamic parameters of metoprolol drug adsorption on the prepared mesoporous silica," *Baghdad Science Journal*, vol. 21, no. 3, 2024.

[16] Diyarov A.A., Mukhamadiev N.Q., Sayitkulov Sh.M., and Uzokov J.R., "Synthesis of mesoporous sorbents on the basis of Al_2O_3 and their textural characteristics," Central Asian Journal of Medical and Natural Science, vol. 3, no. 3, pp. 511-518, May 2022.

[17] H. J. Mohammed and S. H. Kareem, "Effect of Surfactant Type as soft template on Properties of Sol-gel Prepared Mesoporous γ-Alumina," In IOP Conference Series: A Modern Perspective of Technology in Chemistry. IOP Publishing, 2024.

[18] M. P. More et al., "Development of surface engineered mesoporous alumina nanoparticles: drug release aspects and cytotoxicity assessment," *IET Nanobiotechnology*, vol. 11, no. 6, pp. 661–668, 2017.

[19] F. A. Hiawi and I. H. Ali, "Study the adsorption behavior of food colorant dye indigo carmine and loratadine drug in aqueous solution," *Scientific Information Database*., vol.6, no.10, pp.720-730, 2022.

[20] Jr, W. J. Weber and J. C. Morris, "Kinetics of adsorption on carbon from solution," *Journal of the sanitary engineering division*, vol.89, no.2, pp.31-59,1963.

[21] A. V. Dolganov, E. E. Muryumin, O. Y. Chernyaeva, E. A. Chugunova, V. P. Mishkin, and K. N. Nishcev, "Fabrication of new metal-free materials for the hydrogen evolution reaction on base of the acridine derivatives immobilized on carbon materials," *Materials Chemistry and Physics*, vol. 224, pp. 148–155, 2019.

[22] S. K. Dawood and S. H. Kareem, "Comparative study of chemical and green preparation of mesoporous silica," *Baghdad Science Journal*, 2025.

[23] E. W. de Menezes *et al.*, "Ionic silica based hybrid material containing the pyridinium group used as an adsorbent for textile dye," *Journal of colloid and interface science*, vol. 378, no. 1, pp. 10–20, 2012.

[24] K. M. Doke and E. M. Khan, "Equilibrium, kinetic and diffusion mechanism of Cr(VI) adsorption onto activated carbon derived from wood apple shell," *Arabian journal of chemistry*, vol. 10, pp. S252–S260, 2017.

[25] M. Haghighi and A. Khoshfetrat, "Au-O-MWCNTs and TiO_2-O-MWCNTs as efficient nanocarriers for dexamethasone: Adsorption isotherms and kinetic studies," *International Journal of Chemical Engineering*, vol. 2021, pp. 1–19, 2021.

[26] P. Singh, P. K. Maiti, and K. Sen, "Pristine and modified-mesoporous alumina: molecular assistance-based drug loading and sustained release activity," *Bulletin of Materials Science (India)*, vol. 43, no. 1, 2020.

[27] L. É. Uhljar, S. Y. Kan, N. Radacsi, V. Koutsos, P. Szabó-Révész, and R. Ambrus, "In vitro drug release, permeability, and structural test of ciprofloxacin-loaded nanofibers," *Pharmaceutics*, vol. 13, no. 4, p. 556, 2021.

[28] R.-D. Pavaloiu, F. Sha'at, C. Hlevca, M. Sha'at, G. Savoiu, and S. Osman, "Evaluation of drug release kinetics from polymeric nanoparticles loaded with poorly water-soluble APIs," *Ovidius University Annals of Chemistry*, vol. 32, no. 2, pp. 132–136, 2021.

[29] T. M. Albayati and A. A. A. Jassam, "Synthesis and characterization of mesoporous materials as a carrier and release of prednisolone in drug delivery system," *Journal of Drug Delivery Science and Technology*, vol. 53, no. 101176, p. 101176, 2019.

[30] U. Jana, A. K. Mohanty, S. L. Pal, P. K. Manna, and G. P. Mohanta, "Felodipine loaded PLGA nanoparticles: preparation, physicochemical characterization and in vivo toxicity study," *Nano Convergence*, vol. 1, no. 1, 2014.

[31] H. A. Hodali, D. M. Marzouqa, and F. Z. Tekfa, "Evaluation of mesoporous silicate nanoparticles for the sustained release of the anticancer drugs: 5-fluorouracil and 7-hydroxycoumarin," *Journal of Sol-Gel Science and Technology*, vol. 80, no. 2, pp. 417–425, 2016.